Biochimica et Biophysica Acta, 634 (1981) 174—190

BBA 47989

EXPERIMENTAL AND THEORETICAL CONSIDERATIONS OF MECHANISMS CONTROLLING CATION EFFECTS ON THYLAKOID MEMBRANE STACKING AND CHLOROPHYLL FLUORESCENCE

B.T. RUBIN, W.S. CHOW and J. BARBER

ARC Photosynthesis Research Group, Botany Department, Imperial College, Prince Consort Road, London, SW7 2BB (U.K.)

(Received July 21st, 1980)

Key words: Thylakoid membrane stacking; Chlorophyll fluorescence; Cations effect; Van der Waals' force; Electrostatic screening; Energy transfer

Summary

The roles of specific cation binding, charge neutralization and electrostatic screening mechanisms in controlling salt-induced stacking and chlorophyll fluorescence changes in thylakoid membranes are examined in the light of new experimental evidence and theoretical calculations of the forces between membrane surfaces. A comparison of the biphasic stacking and fluorescence phenomena generated by organic mono- and divalent cations known sterically to inhibit specific binding with the effects generated by inorganic mono- and divalent cations suggests that the observed salt-induced changes at pH $\geqslant$ 7.5 are predominantly governed by the electrostatic screening mechanism in agreement with previous work (e.g. Barber, J., Mills, J.D. and Love, A. (1977) FEBS Lett. 74, 174—181). Detailed calculations of the coulombic double layer repulsive force between negatively charged membrane surfaces immersed in a mixed electrolyte of valence type Z^{1+}/Z^{1-},Z^{2+}/Z^{1-} were performed both under the constraints of fixed surface charge density and fixed surface potential. From a close comparison of the theoretical results with new experimental data on salt-induced stacking and fluorescence changes and a consideration of the contributions of the 'hydration' repulsive force and the van der Waals attractive force, it is argued that a reduction in surface charge density alone by lateral diffusion is probably insufficient to realize membrane stacking and that an increase in the van der Waals attractive force is necessary to account for the experimental observations perhaps through the formation of protein rich domains. In view of the complexity of the thylakoid membranes, the conclusions are to be considered qualitative. Nevertheless, these calculations give support to a model in which the cation induced chlorophyll fluorescence and stacking changes can be explained by lateral diffusion of two types of pigment protein complexes in the

lipid matrix of the membrane. Such diffusion gives rise to changes in energy transfer between Photosystem II and Photosystem I and also to the creation of domains having low and high electrical surface charge density.

Introduction

The stacking, chlorophyll fluorescence yield and electron transport properties of isolated chloroplast thylakoids have been shown to be sensitive to the ionic content of the suspension medium [1—4]. Characteristic changes in these properties generated by cations having different valencies and by an antagonism between low concentrations of divalent and monovalent cations [5—10] have led Barber et al. [7]] to postulate that the controlling mechanism involves electrostatic screening of negative charges on the thylakoid surface. Such screening will result in a reduction of the coulombic repulsion between surfaces and bring about conformational changes both in and between membranes [11—14]. However, in addition to electrostatic screening, coulombic repulsion between surfaces will be reduced if specific cation binding or protonation occurs in such a way as to lower the surface charge density [14.15]. In particular, under low salt conditions, when there is a substantial negative surface potential, the local concentration of cations, including H^+, will be high and charge neutralisation possible. For example, Duniec et al. [14] and Sculley et al. [15] have considered this possibility in their theoretical consideration of thylakoid stacking.

In this paper we continue to explore the role of electrostatic screening as being the main controlling parameter for salt-induced thylakoid stacking and chlorophyll fluorescence yield changes. We have carried out experiments under a variety of mixed electrolyte conditions and used not only inorganic, but organic cations with the view to minimising ion binding to the membrane surface. Theoretical analyses of the results have been made by taking into account not only the electrostatic repulsive forces, but also contributions of the van der Waals attractive and hydration repulsive forces. Calculations of electrostatic repulsion have been performed both under the constraints of fixed surface charge density and fixed surface potential. The latter case permits free surface charge displacement in the plane of the membrane. The relevance of these results is briefly discussed in terms of a model to explain the relationship between thylakoid stacking and chlorophyll fluorescence changes [13,16—18].

Materials and Methods

Experimental

Envelope-free chloroplasts were prepared from pea leaves as described in Ref. 17 in the unstacked or stacked form by including 0.1 mM ethylenediamine tetraacetate (EDTA) or 1 mM $MgCl_2$, respectively, in the wash medium. For Fig. 1, 2 mM decamethorium bromide (*N,N,N,N',N',N'*-hexamethyl-1,10-decanediaminium dibromide) was used in the wash medium instead of $MgCl_2$. The chloroplast stock was kept in the respective wash medium on ice at a chlorophyll concentration of 3 to 5 mg/ml, and aliquots were diluted into a required salt medium just before use.

Chlorophyll fluorescence was excited using blue light of intensity 10 W/m^2 in the presence of 10 μM 3-(3,4-dichlorophenyl)-1,1-dimethylurea (DCMU), while the relative degree of thylakoid membrane stacking was monitored by the chlorophyll content of a 10 000 $\times$ g pellet following digitonin treatment, as previously described [17]. The basic medium containing 100 mM sorbitol, 1 mM N-2-hydroxyethylpiperazine-N'-2-ethanesulphonic acid (Hepes) (pH 7.5, KOH) was supplemented by the various salt concentrations as indicated. When an essentially salt-free medium was required, a 100 mM sorbitol solution was brought to pH 7.5 with Tris buffer (about 0.1 mM). All samples were pre-incubated in the various salt regimes for 8 to 10 minutes at room temperature before chlorophyll fluorescence measurement or digitonin treatment.

Theoretical

Calculations of the electrostatic double layer repulsive force (P) between identical negatively charged membrane plates were performed using the full non-linear Poisson-Boltzmann equation both under the constraints of constant surface density and constant surface potential. The numerical methods for the calculation were similar to those employed by Hall [19] and Hall and Sculley [20], the details of which are given in the Appendix. The parameters used for the various calculations were as follows: T = 298.16 K, ϵ = 78.4, σ = —0.025 C/m^2, where T is the thermodynamic temperature, ϵ is the dielectric constant of the electrolyte medium and σ is the membrane surface charge density. In the calculation of the repulsive force at constant charge density a uniform charge distribution was assumed. In the calculation of the double layer repulsive force at constant surface potential, a uniform charge distribution was assumed at infinite plate separation with a surface charge density of —0.025 C/m^2. The computer-generated force curves for membranes immersed in a mixed electrolyte having valence types Z^{1+}/Z^{1-},Z^{2+}/Z^{1-} were calculated as a function of plate separation distance x_p ($1.0 \leqslant x_p \leqslant 8.0$ nm) for various combinations of mono- and divalent salt conditions corresponding to those used in the experiments.

These calculations of electrostatic forces were compared with the values of van der Waals and hydration forces taken from the recent paper of Sculley et al. [15]. In their paper they used an expression derived by Parsegian and Ninham [21] for calculating van der Waals interactions between two flat membrane surfaces composed of various amounts of lipid and protein each with different dielectric constants. For estimation of hydration repulsive forces, Sculley et al. [15] used an empirical formula previously employed by others [22, 23].

Results

Experimental

Fig. 1 shows the effect, on thylakoid stacking (measured as described in Materials and Methods) and chlorophyll fluorescence, of increasing the level of choline chloride in the suspension medium. In this experiment the membranes had been prewashed with a low level of EDTA to remove inorganic divalent cation and simultaneously treated with a low level of the divalent organic cation, decamethonium. It is apparent that the same general qualitative

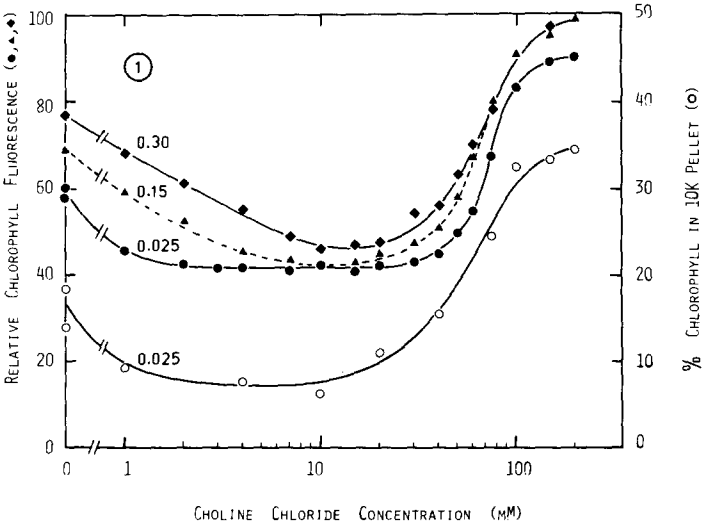

Fig. 1. Effects of increasing choline chloride concentration on thylakoid stacking (○———○) and chlorophyll fluorescence (solid symbols) in the presence of a given background concentration of decamethonium dibromide (indicated in mM).

behaviour is observed with both organic and inorganic cations (see Fig. 2). Fig. 2 also shows the important property of the two salt-induced phenomena, that the effectiveness of low levels of monovalent cation to induce unstacking and decrease chlorophyll fluorescence is reduced when the background level of divalent cation is increased. Also there is a shift of the minimum towards high monovalent concentrations.

The unstacked/low fluorescence state occurs over a reasonably large monovalent cation range (approx. 1—30 mM) when the background divalent cation level is low. Addition of divalent cations to the suspension brings about restacking and a return to the state of high fluorescence yield. As Fig. 3 shows, the concentration of divalent cations required to bring about these effects is dependent on the background level of monovalent cation. These curves may be characterised by their 'cross-over' values which can be described in terms of the order of intersection of the curves along the vertical axis ($c_2 = 0$) and the asymptotic order of the curves in the plateau region ($1.5 \leqslant c_2 \leqslant 5$ mM) with respect to their projected values on the vertical axis. Thus in Fig. 3A the intersections on the vertical axis are in the order $50 > 10 > 1$ mM while the asymptotic order of the plateaux is reversed to $1 > 10 > 50$ mM. A similar behaviour in these quantities is displayed in Fig. 3B.

Theoretical

The calculated results for the double layer repulsive force at constant surface charge density (P_σ) and constant surface potential (P_{ψ_s}) are shown in Figs. 4 and 5 respectively. The electrolyte concentrations were selected to match the experimental regime of measurements displayed in Figs. 2 and 3.

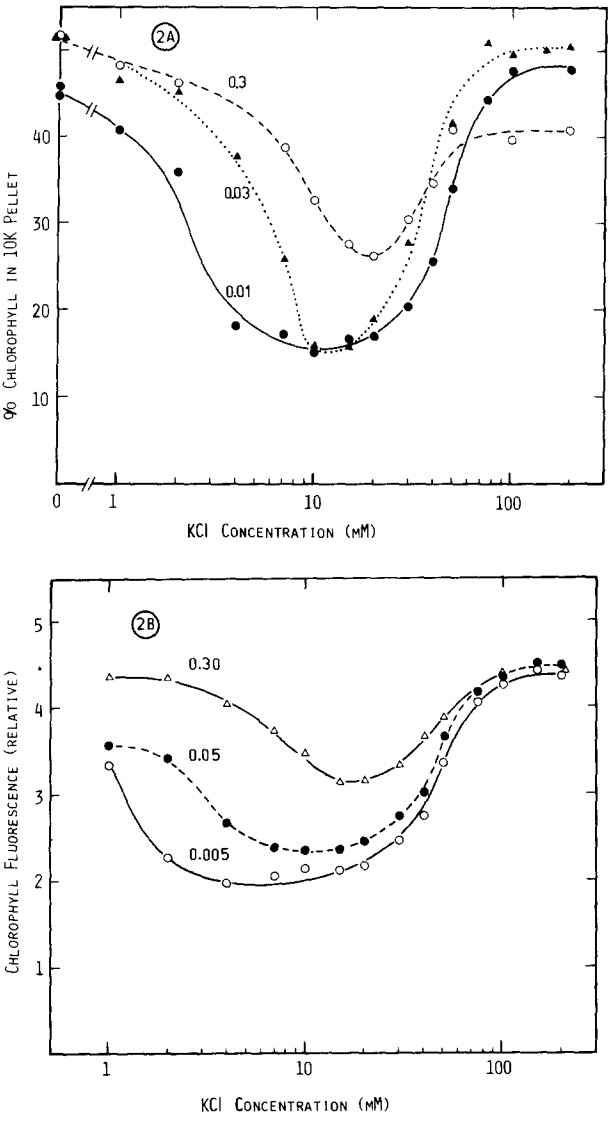

Fig. 2. Effects of increasing KCl concentrations on thylakoid stacking (A) and chlorophyll fluorescence (B) in the presence of a given background concentration of $MgCl_2$ (indicated in mM).

Fig. 4A shows computer derived curves for the force P_σ as a function of monovalent cation concentration c_1 at three background divalent cation concentration levels c_2 and at three plate separation distances. The P_σ vs. c_1 curves at various fixed background levels of c_2 at a given separation distance x_p display a maximum which corresponds to the minimum in the experimental curves shown in Fig. 2A and 2B. The maximum regions in P_σ thus correspond to unstacking and low fluorescence values. The lower values of P_σ correspond to membrane stacking and high relative fluorescence values. Further, the maxima in P_σ at a given x_p shift to higher values along the monovalent cation con-

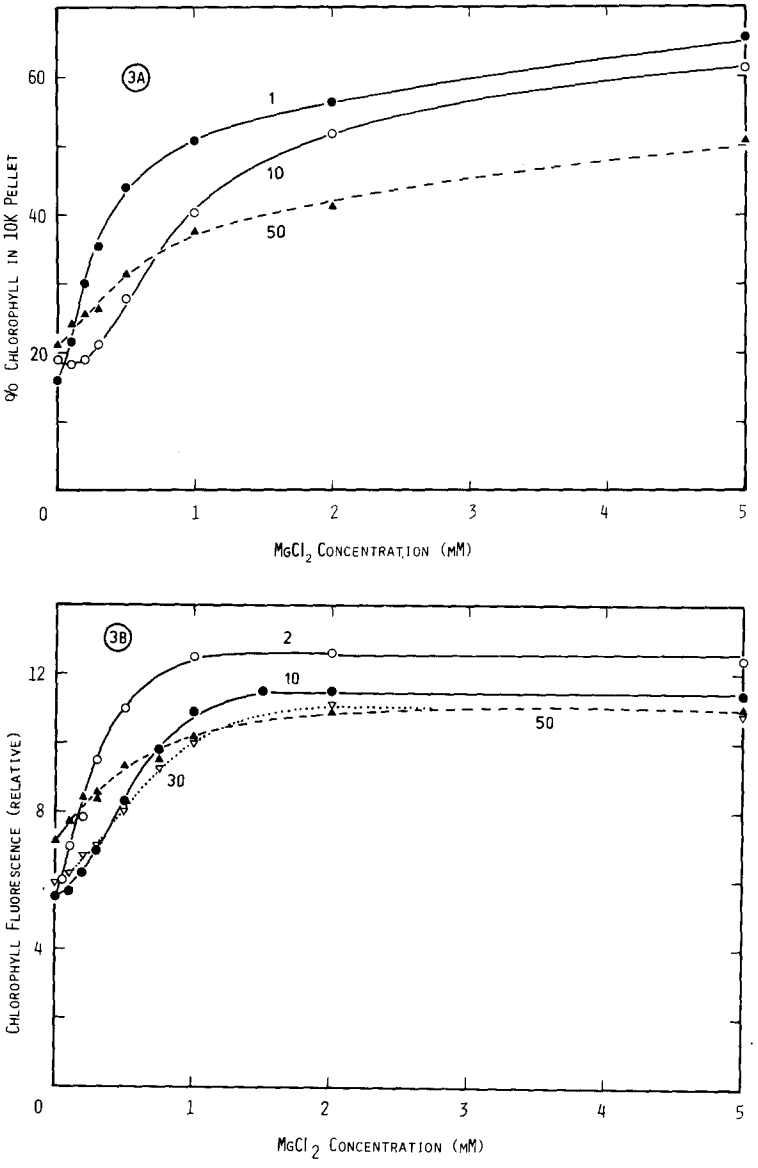

Fig. 3. Effects of increasing $MgCl_2$ concentration on thylakoid stacking (A) and chlorophyll fluorescence (B) in the presence of a given background concentration of KCl (indicated in mM).

centration axis with increasing background divalent cation concentration level in agreement with the experimental behaviour depicted in Figs. 2A and 2B. Finally, the maxima in P_σ shift to higher values along the monovalent cation concentration axis as the plate separation decreases.

Fig. 4B displays the plate separation at distance x_p = 1.5 nm at which the curves for the force P_σ vs. divalent cation concentration best match the experimental behaviour depicted in Fig. 3A. The 'cross-over' criteria described in Experimental Results are fully satisfied by the theoretical curves, though

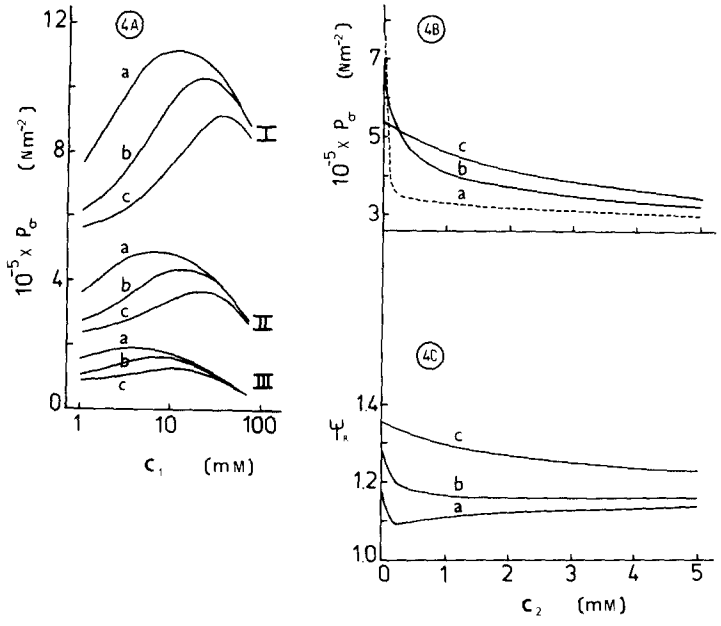

Fig. 4. A shows the double layer repulsive force at constant surface charge P_σ as a function of monovalent concentration level c_1 at three background divalent concentration levels (a = 0.005, b = 0.05, c = 0.3 mM) and at three membrane plate separation distances x_p (I = 1.0, II = 2.0, III = 4.0 nm). B and C show, respectively, the double layer repulsive force P_σ and the corresponding surface potential ratio ψ_R as a function of divalent concentration level at three background monovalent concentration levels (a = 1, b = 10, c = 50 mM) at the membrane plate separation distance x_p = 1.5 nm.

clearly both the intersections and the projected asymptotic values on the P_σ axis are in the reverse order of that found in Fig. 3A since a high value of P_σ corresponds to unstacking and low chlorophyll content in the 10 000 × g pellet.

Fig. 4C exhibits the surface potential ratio ψ_R corresponding to the salt conditions and separation distance of Fig. 4B. The behaviour of ψ_R does not satisfy the measured 'cross-over' criteria (ψ_R is defined as the surface potential ψ_s at a given plate separation distance divided by the surface potential at infinite plate separation ψ_s^∞).

Fig. 5A shows computer derived curves for the double layer repulsive force P_{ψ_s} at constant surface potential ψ_s as a function of monovalent cation concentration c_1 at three background divalent cation concentration levels c_2 and for three plate separation distances. The P_{ψ_s} vs. c_1 curves at various fixed background c_2 levels at a given x_p display maxima which correspond to the minima manifest in experimental curves in Fig. 2 A and B. Further, maxima in P_{ψ_s} at a given x_p shift to higher values along the c_1 axis with increasing background levels of c_2 in agreement with the experimental data shown in Fig. 2 A and B. Finally, maxima in P_{ψ_s} shift to higher c_1 values as x_p decreases for a given c_2.

In Fig. 5B, the P_{ψ_s} curves at x_p = 1.0 nm satisfy the experimental 'cross-over' criteria of Fig. 3A. The corresponding behaviour of the surface charge ratio σ_R given in Fig. 5C indicates that the 'cross-over' criteria are similarly satisfied (σ_R

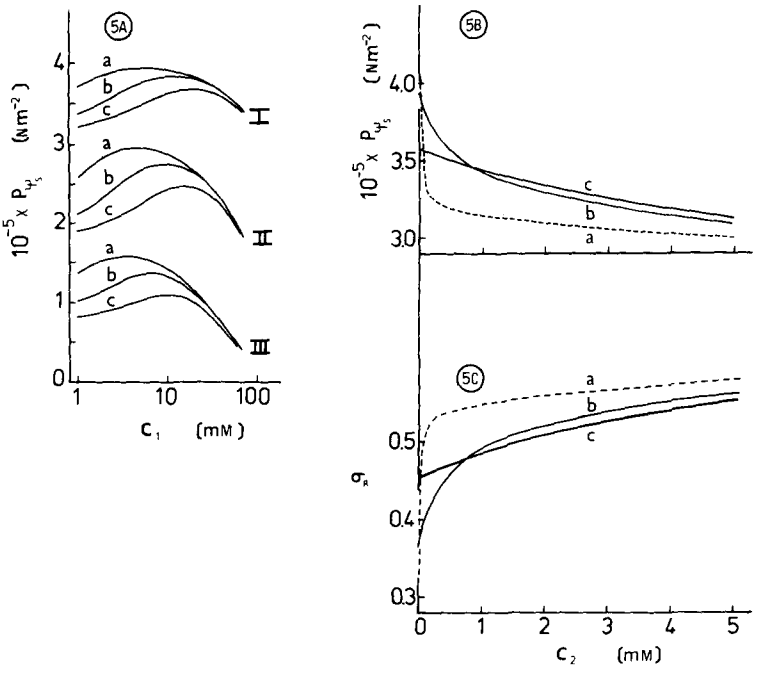

Fig. 5. A shows the double layer repulsive force at constant surface potential P_{ψ_s} as a function of monovalent concentration level c_1 at three background divalent concentration levels (a = 0.005, b = 0.05, c = 0.3 mM) and at three membrane plate separation distances x_p (I = 1.0, II = 2.0, III = 4.0 nm). B and C show, respectively, the double layer repulsive force P_{ψ_s} and the corresponding surface charge ratio σ_R as a function of divalent concentration level at three background monovalent concentration levels (a = 1, b = 10, c = 50 mM) at the membrane plate separation distance x_p = 1.0 nm.

is defined as the value of the surface charge density at a given plate separation distance divided by the surface charge density at infinite plate separation (σ_∞ = −0.025 C/m^2) for the same set of salt conditions). The σ_R curves follow the inverse behaviour of the force curves P_{ψ_s}.

Comparison of Figs. 4 and 5 indicate that over the same range of separation distance considered $P_\sigma > P_{\psi_s}$; that the maxima in P_σ vs. c_1 curves occur at higher c_1 values than the corresponding maxima in the P_{ψ_s} vs. c_1 curves; that in Fig. 4B the P_σ vs. c_2 curves satisfy the experimental 'cross-over' criteria at x_p = 1.5 nm whilst the corresponding values of ψ_R shown in Fig. 4C do not; that both P_{ψ_s} and σ_R vs. c_2 curves shown, respectively, in Figs. 5C and 5D satisfy the measured 'cross-over' criteria at x_p = 1.0 nm. The rationale implicit in the comparison of theoretical and experimental results is developed in the Discussion.

Fig. 6A illustrates typical asymptotic behaviour of σ_R with increasing x_p at four values of c_1 for one fixed background c_2 level. Fig. 6B exhibits the asymptotic behaviour of σ_R with increasing x_p at three values of c_2 for one fixed background c_1 level. Both figures indicate that σ_R decreases with decreasing x_p under the assumption of constant surface potential.

Fig. 7 shows curves of P_σ and P_{ψ_s} plotted as a function of x_p for two typical sets of salt conditions. At very close plate separation distances P_σ exceeds P_{ψ_s}

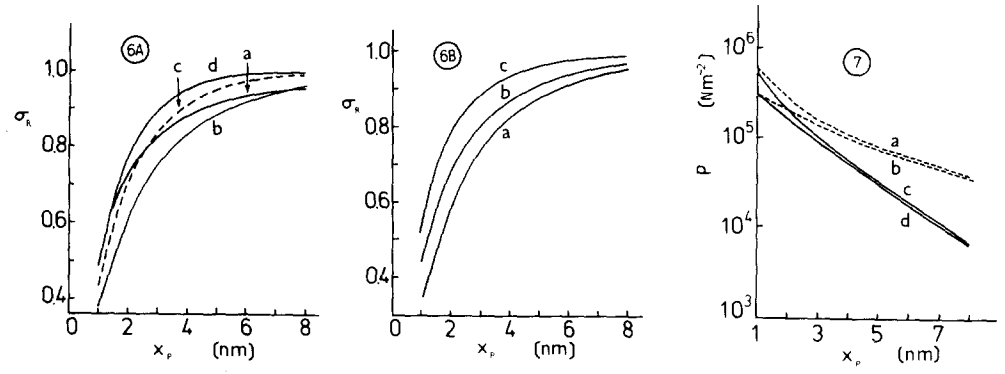

Fig. 6. A and B show, respectively, the surface charge ratio σ_R at constant surface potential as a function of membrane plate separation distance x_p for two sets of salt conditions. In A the divalent concentration level is fixed at c_2 = 0.05 mM whilst the monovalent concentration levels c_1 are indicated as: a = 1, b = 10, c = 40, d = 70 mM. In B the monovalent concentration level is fixed at c_1 = 10 mM whilst the divalent concentration levels c_2 are indicated as: a = 0.0, b = 0.4, c = 5.0 mM.

Fig. 7. The double layer repulsive force at constant charge P_σ and at constant surface potential P_{ψ_s} as a function of membrane plate separation distance x_p for two sets of salt conditions. Curves a and b represent, respectively, the forces P_σ and P_{ψ_s} calculated for the salt condition: c_1 = 1 mM, c_2 = 0.05 mM. Curves c and d represent respectively the forces P_σ and P_{ψ_s} calculated for the salt condition: c_1 = 10 mM, c_2 = 5 mM.

but as x_p increases the difference between P_σ and P_{ψ_s} diminishes. This behaviour is in agreement with previous double layer force calculations [24].

Discussion

The role of specific cation binding in controlling salt-induced stacking of thylakoid membranes and related chlorophyll fluorescence phenomena may be evaluated by comparison of Figs. 1 and 2. The organic choline and decamethonium cations bear mono- and divalent charges electrically equivalent to the inorganic potassium and magnesium cations. However, the organic cations are likely to be sterically hindered from close approach to the membrane surface thus severely limiting the extent of specific binding with the negatively charged groups at the surface [25]. The general qualitative agreement between Figs. 1 and 2 indicates that although potassium and magnesium ions may bind to some extent, the biphasic behaviour of salt-induced stacking and fluorescence changes is preserved. This conclusion is in line with previous findings that these cation-induced phenomena showed little or no specificity to a range of cations within the same valency group [8,10,16]. Theoretical curves presented in Figs. 4A and 5A exhibit biphasic behaviour which correlates well with the experimental measurements. Maxima in the force vs. concentration curves correspond to the observed minima seen in Fig. 2 A and B. The theoretical curves tend to follow the biphasic behaviour induced by the inorganic cations more closely than that induced by the sterically hindered organic cations. An extended 'minimum' region in the case of organic cations is apparent and may be due to the effects of non-uniform charge distribution on the organic cations,

increased cation size and decreased membrane permeability. Since the experiments were carried out at pH 7.5, the contribution of neutralization of surface charge by protonation is considered negligible [26—28]..Consequently, the dominant mechanism controlling thylakoid stacking and chlorophyll fluorescence changes under these experimental conditions would appear to be the electrostatic screening mechanism in agreement with previous work [7,8,10—12].

In attempting to explore the effects of the electrostatic screening mechanism in further detail, theoretical curves for the double layer repulsive force between semi-infinite membrane plates have been generated and compared directly with experimental observations in Fig. 3A. The underlying initial assumptions which such a comparison requires is that the contributions of all remaining forces including both the van der Waals attractive force arising from the interaction of composite lipoprotein membrane surfaces and the repulsive hydration force arising from 'structured water' be essentially independent of salt concentration changes. The independence of the van der Waals force and the hydration force on electrolyte concentration was implicitly assumed in the work of Sculley et al. [15]. The validity of this assumption is discussed below. For the purpose of developing the following arguments only the double layer repulsive force is assumed to be sensitive to concentration changes in the electrolyte. It is further assumed that variations in the total chlorophyll content in the 10 000 × *g* digitonin derived pellet reflects a fairly direct measure of the total net force operating between thylakoid membranes (see Ref. 10). If this is the case, then to a first approximation, the electrolyte-dependent contribution to the total force will be proportional to the double layer repulsive force. Another aspect affecting the comparison of theory and experiment is the choice of surface charge density. A variety of experimental methods [26—30] bracket the range of the surface charge density such that $0.008 \leqslant |\sigma| \leqslant 0.053$ C/m^2. Thus the choice of an average value of $\sigma = -0.025$ C/m^2 is reasonable and in line with other studies [7]. Also worthy of note is that at pH $\geqslant$ 7.5 the net charge on the thylakoid surface is essentially due to negatively charged residues on the exposed segments of integral membrane protein complexes [27,31,32].

The carefully controlled measurements depicted by the curves in Fig. 3A provide a basis for close comparison with the theoretical results presented in Figs. 4B, 4C, 5B and 5C. It is apparent that all the qualitative features of the 'cross-over' curves displayed in Fig. 3A are manifest in the theoretical curves shown in Figs. 4B, 5B, 5C. The matching of the theoretical force curves with experimental observations occurs in P_σ at $x_p = 1.5$ nm and in P_{ψ_s} at $x_p = 1.0$ nm. These results are not arbitrary since at significantly different separation distances the force curves (not shown) do not satisfy the matching 'cross-over' criteria. The results also indicate that the surface potential ratio ψ_R given in Fig. 4C does not satisfy the matching criteria at $x_p = 1.5$ nm wheras the surface charge density ratio σ_R given in Fig. 5C at $x_p = 1.0$ nm does. The fact that a match of the experimental data could be obtained is supportive of the underlying assumptions in this analysis and moreover emphasises the close correlation between electrostatic screening effects and salt-induced membrane stacking and fluorescence changes.

Electron micrographs [33] suggest that the in vivo separation distance

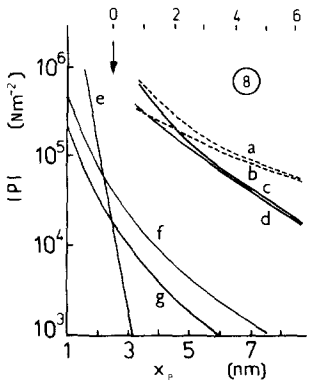

Fig. 8. The absolute value of each contribution of the force P between membrane plates as function of membrane plate separation x_p. Curves a, b, c, d represent the double layer repulsive forces P_σ and P_{ψ_s} under two sets of salt conditions as shown in Fig. 7. These curves have been transposed from Fig. 7 to Fig. 8 and repositioned relative to the separation distance between outer Helmholtz planes as is indicated in the upper scale. The position of the arrow denotes zero plate separation between the outer Helmholtz planes. Curves e, f, g have been reproduced from the work of Sculley et al. [15]. Curve e represents the contribution of the hydration repulsive force whilst curves f and g represent the contribution of the van der Waals attractive force corresponding to two different dielectric constants of 3 and 2.5 with respective volume fractions of protein to lipid in the membrane of 0.6 and 0.4.

between stacked thylakoid membranes occurs in the range of $x_p \simeq 4.0$ nm. In order to obtain theoretical matching of the measured 'cross-over' curves at this plate separation distance surface charge densities far higher than measured had to be assumed in the theoretical calculations. Thus, the electron micrographic evidence requiring $x_p \simeq 4.0$ nm for stacked membranes and the good agreement of the theoretical curves with the experimental data obtained at x_p in the range $1.0 \leqslant x_p \leqslant 1.5$ nm lead to an apparent contradiction. This discrepancy is resolved if allowance is made for the effect of the hydration repulsive force whose origin is associated with structured water near the membrane surface which is different from bulk water. In certain circumstances the effect of 'surface hydration' may extend to distances as much as 2.5 nm from a charged surface [34]. Thus the plate separation distances x_p employed in the double layer repulsive force calculations apply rigorously only to the region separating the membrane plates, where the normal structure of water occurs and Poisson-Boltzmann statistics apply. This region is bounded by the outer Helmholtz planes of the membrane plates. Consequently, the outer Helmholtz plane is set at a distance from the membrane plate surface at which the hydration repulsive force is significantly reduced. In Fig. 8 the contributions of both the hydration repulsive force and the van der Waals attractive force are reproduced from the work of Sculley et al. [15]. From the curve e it is evident that the hydration repulsive force falls below other contributions at $x_p \geqslant 2.5$ nm. Using this value the electrostatic double layer repulsive force curves of Fig. 7 have been transposed to Fig. 8 taking into account the approximate positioning of the outer Helmholtz plane relative to the 'geometrical' membrane plate surface. The outer Helmholtz plane is thus located at a distance of $\simeq 1.25$ nm from each membrane plate surface. This repositioning of the double layer force curves

removes the apparent contradiction and gives a result of an overall 'geometrical' plate separation in the range 3.5—4.0 nm in agreement with electron micrographic data. In these calculations the outer Helmholtz plane represents the 'effective' uniform charge bearing plane whereas the position of the 'actual' charge bearing plane due to charged proteins is located within the region bounded by the 'geometrical' membrane plate surface and the outer Helmholtz plane. The actual position of the outer Helmholtz plane is to be regarded as approximate since it is likely that the constant charge assumption in the calculation of P_σ and the constant potential assumption in the calculation of P_{ψ_s} may imply different contributions of the hydration repulsive force.

The van der Waals force calculations were performed for membranes consisting of a randomly oriented mixture composed of proteins embedded in a lipid matrix according to Sculley et al. [15]. The results represent a band of values delineated by curves f and g in Fig. 8 and correspond to two different dielectric constants of 3 and 2.5 with volume fractions of protein to lipid respectively in the range 0.6 to 0.4. As can be seen from Fig. 8 the band of van der Waals attractive forces falls well below the coulombic double layer repulsive force curves which are given for two typical sets of salt conditions. The calculation of the force P_{ψ_s} at constant potebtial allows for a decrease in surface charge density as x_p decreases. Such a decrease in surface charge density as illustrated in Fig. 6 may occur by lateral diffusion of charge away from membrane regions in close apposition [12,35,36]. Comparison of curve d in Fig. 8 with the corresponding curve for σ_R in Fig. 6B indicates a drop in σ_R to $\simeq 0.56$ at a separation distance of 1.0 nm between outer Helmholtz planes. This minimum value of σ_R is still sufficiently high (i.e. -0.014 C/m^2) such that the double layer repulsive contribution exceeds the van der Waals attractive contribution. However, the relative difference between these contributions would be somewhat reduced if the neutral surface of charge bearing membrane proteins protrude significantly into the aqueous phase beyind the outer Helmholtz plane. The extent of this effect requires further theoretical treatment. However, if the exposed protein surfaces are confined within the space between the 'geometrical' membrane plate surface and the outer Helmholtz plane, then the shift of the van der Waals contribution along the distance axis of Fig. 8 may be insufficient to overlap the double layer repulsive contribution. Hence, in this case, it is necessary to consider an increase in the van der Waals attractive force, possibly generated by the formation of protein rich domains, which together with the decrease in charge density due to lateral charge displacement allows a stable balance of repulsive and attractive forces to occur at the required separation distance between the two surfaces. As a consequence the van der Waals contribution in Fig. 8 would then be shifted upwards along the force axis so as to overlap the double layer repulsive contribution. This reasoning differs from that of Sculley et al. [15] who assumed unrealistically low values of the surface charge density, $|\sigma| \leqslant 5.3 \cdot 10^{-3}$ C/m^2 in order to reduce the double layer repulsive contribution to within the range of the van der Waals contribution. In addition, reduction of surface charge density by lateral diffusion was not analyzed in their model.

The mechanism envisaged for increasing the van der Waals contribution is based upon the removal of the constraint imposed by a random distribution of

proteins in the lipid matrix. Once the proteins are considered sufficiently mobile, the formation of protein rich domains by lateral diffusion enhanced by the cooperative effects between two or more membrane surfaces may occur. In this regard the recent theoretical study of Weinbaum [37] on the formation of intercellular tight junctions is particularly relevant. The increase in the van der Waals attractive force suggested by the present analysis lends support to recent models [12,13] proposed for the explanation of salt-induced thylakoid stacking and fluorescence changes [13,16—18]. In these models the lateral movement of different types of chlorophyll-protein complexes, and possibly of non-pigmented complexes is thought to occur when electrostatic screening is increased so that protein-rich domains form having either high or low surface charge densities. It is argued that it is the partial segregation of different pigment-protein complexes (fluorescing Photosystem II and quenching Photosystem I) which gives rise to the changes in fluorescence yield and which creates the heterogeneity on the membrane surface [38] responsible for granal (stacked) and stromal (unstacked) membranes.

In the analyses presented in this paper no correction was made for the variation of electrolyte concentration in the van der Waals force and the hydration repulsive force. Theoretical work suggests that the effect of increased ionic strength is to damp the zero frequency contribution to the van der Waals force which under certain conditions may result in a significant reduction (as much as 50%) in this force [39]. The direction of this effect would tend to favour the requirement for enhanced domain formation. In the case of the repulsive hydration force, experimental observations suggest an exponential decay with distance which is essentially independent of electrolyte composition [22,23,34]. The assumptions underlying the potential of mean force implicit in the use of the Poisson-Boltzmann equation for double layer force calculations have been the subject of a statistical mechanical treatment [40]. The results indicate how the Gouy-Chapman approximation of the potential of mean force, i.e. the potential due to the charged plate but screened by the ions in solution, may be represented by the sum of an interionic potential term and the unscreened external potential. However, the use of the Poisson-Boltzmann equation does not take into account the structure making and breaking effects of the ions on the supporting aqueous solvent. The assumption of a uniform 'smeared' charge distribution in the calculations deserves some attention in the circumstances when the plate separation distance is comparable to the average separation of charges on the surfaces. The consequences arising from the interaction of discrete charge distributions modelled as parallel planar arrays of like charges distributed over square lattices may be assessed from Richmond's calculations [41]. His results (see Ref. 41, p. 1159) indicate that at relevant plate separations, a higher repulsive force than that generated by the corresponding uniform 'smeared' charge distribution occurs, when the positions of the lattice charges in each planar array are directly opposite. To achieve a stable balance of forces, a higher repulsion arising from the discreteness of charge would require an even greater van der Waals attraction. A shift of one lattice relative to the other at a given separation distance leads to a reduction in the repulsive component which approaches that of the smeared charge distribution. Since membranes are not rigid plates, and since the protein bearing charges are con-

sidered mobile, it is likely that the most energetically favoured relative displacement of like charged apposed membrane plate arrays would be that corresponding to minimum repulsion which approaches the repulsive force generated by the uniform 'smeared' charge distribution.

Finally, it should be pointed out that because of the various assumptions made in the calculations the conclusions are to be regarded with some caution. Nevertheless, the analysis emphasises the interplay between repulsive and attractive forces between membrane surfaces under mixed electrolyte conditions. Morever, the treatment highlights the possible importance of charge displacement and increased van der Waals attraction in membrane domain formation and thus the direction of further studies.

Acknowledgement

The authors are indebted to Dr. L. Le N. McFarlane for considerable programming assistance in implementing the numerical computational techniques. We thank the Science Research Council for financial support.

Appendix

The force (P) between identical semi-infinite parallel charged plates immersed in a mixed electrolyte of valence type $Z^{1+}/Z^{1-}, Z^{2+}/Z^{1-}$ was calculated by solving the one-dimensional Poisson-Boltzmann equation in the region between the plates, i.e.

$$d^2\psi/dx^2 = -(1/\epsilon_0\epsilon) \sum_i z_i F c_i \exp(-z_i F\psi/RT) \tag{1}$$

where ψ is the electrostatic potential; x is the distance; z_i is the valence of the i-th ion; c_i is the concentration of the i-th ion; ϵ_0, ϵ are, respectively, the permittivity of free space and the dielectric constant of the electrolyte medium; F is the Faraday constant, R is the molar gas constant; and T is the thermodynamic temperature. From symmetry considerations, Eqn. 1 is solved in one half the region between the plates subject to boundary conditions at one plate surface and at the midplane separating the two parallel plates, i.e.

$$\sigma = -\epsilon_0\epsilon(d\psi/dx)_{x=s} \tag{2}$$

$$(d\psi/dx) = 0\,, \qquad \psi = \psi_m \tag{3}$$

where σ is the surface charge density on the plate surface located at a distance $x = s$ from the midplane; ψ_m is the midplane potential located half way between the plates. Eqn. 1 may be integrated once yielding the results

$$(d\psi/dx)^2 = (2RT/\epsilon_0\epsilon) \sum_i c_i[\exp(-z_i F\psi/RT) + C^*] \tag{4}$$

where C^* is the integration constant. Employing Eqn. 4, Eqn. 2 may be written as:

$$\sigma^2 = 2RT\epsilon_0\epsilon \sum_i c_i[\exp(-z_i F\psi_s/RT) + C^*] \tag{5}$$

where ψ_s is the potential at the surface of the plate.

Using Eqns. 3 and 4 the integration constant is written as:

$$C^* = -\sum_i c_i \exp(-z_i F\psi_m/RT)/\sum_i c_i \tag{6}$$

Substituting Eqn. 6 into Eqn. 5 one obtains:

$$\sigma^2 = (2RT\epsilon_0\epsilon)\left\{\sum_i c_i \exp(-z_i F\psi_s/RT) - \sum_i c_i \exp(-z_i F\psi_m/RT)\right\} \tag{7}$$

At infinite plate separation ($x \to \infty$), $\psi_m \to 0$, and Eqn. 7 reduces to the expression for an isolated plate in electrolyte medium:

$$\sigma_\infty^2 = (2RT\epsilon_0\epsilon)\left\{\sum_i c_i[\exp(-z_i F\psi_s^\infty/RT) - 1]\right\} \tag{8}$$

where σ_∞, ψ_s^∞ are, respectively, the surface charge density and surface potential at infinite plate separation. Eqn. 4 may be integrated once more giving the plate separation distance x_p as function of ψ_s and ψ_m:

$$x_p = \{2/(2RT/\epsilon_0\epsilon)^{1/2}\}\int_{\psi_m}^{\psi_s} d\psi/\{\sum_i c_i \exp(-z_i F\psi/RT) - \sum_i c_i \exp(-z_i F\psi_m/RT)\}^{1/} \tag{9}$$

where Eqn. 6 has been used. Finally, the force is calculated from the general expression

$$P = -RT\sum_i c_i(C^* + 1) \tag{10}$$

where C^* is determined from Eqn. 6 once ψ_m is known. Eqns. 7 through 10 are utilized to calculate the force between the plates both under the constraint of constant surface potential and constant surface charge density.

Constant surface potential

For a given set of salt conditions Eqn. 8 is solved for ψ_s^∞ assuming a surface charge density at infinite plate separation $\sigma_\infty = -0.025$ C/m^2. Assuming a given separation distance x_p, and setting the upper limit in Eqn. 9 such that $\psi_s = \psi_s^\infty$, the integral is evaluated by iterating ψ_m over a range of values until the right-hand side of Eqn. 9 equals the given value of x_p on the left-hand side to within a predetermined accuracy. The values of ψ_s^∞, ψ_m which satisfy Eqn. 9 are then substituted back into Eqn. 7 to determine σ at the given separation distance x_p and the ratio $\sigma_R = \sigma/\sigma_\infty$. Finally, the value of ψ_m obtained is used to calculate C^* from Eqn. 6 and the result employed to determine the force P_{ψ_s} from Eqn. 10. The subscript ψ_s indicates constant surface potential.

Constant surface charge density

For a given set of salt conditions Eqn. 9 is solved as function of ψ_s, ψ_m subject to the constraints imposed on ψ_s, ψ_m by Eqn. 7 with constant surface charge density assumed to be: $\sigma = -0.025$ C/m^2. A Newton-Raphson type of shooting technique is employed which involves iterating ψ_s and calculating the corresponding values of ψ_m from Eqn. 7. A set of iterative values for the right-hand side of Eqn. 9 is obtained and the procedure terminates when the right-

hand side converges to a specified value of x_p within a predetermined accuracy. The value of ψ_s which serves as lower bound to initial estimates of ψ_s in the shooting technique is found from Eqn. 8 whence $\psi_s = \psi_s^\infty$ with $\sigma_\infty = -0.025$ C/m^2. The efficiency of convergence of the right-hand side of Eqn. 9 is sensitive to the initial values of ψ_s, ψ_m determined from Eqn. 7 whereupon a threshold value of ψ_m was assumed. Once convergence is obtained, the corresponding values of ψ_s, ψ_m are substituted back into Eqn. 7 as a final check. At a given separation distance the ratio $\psi_R = \psi_s/\psi_s^\infty$ is calculated and finally the force P_σ is calculated using Eqns. 6 and 10 with the previously determined value of ψ_m. The subscript σ indicates constant surface charge density.

In both the cases of constant surface potential and constant surface charge density the singularity apparent in the improper integral in Eqn. 9, which occurs when $\psi = \psi_m$ in the integrand is dealt with by standard numerical technique. From a consideration of the behaviour of the integrand in the neighbourhood of the singularity, the lower limit of integration is set as $\psi = \psi_m + \xi$ where ξ is a small number. Convergence is obtained by letting ξ tend to zero for a given pair of integration limits (ψ_s, ψ_m). Similar procedures have been employed in other treatments [19,20].

References

1 Anderson, J.M. (1975) Biochim. Biophys. Acta 416, 191—235
2 Barber, J. (1976) in The Intact Chloroplast, Vol. 1, Topics in Photosynthesis (Barber, J., ed.), pp. 89—134, Elsevier/North Holland, Amsterdam
3 Williams, W.P. (1977) in Primary Processes in Photosynthesis, Vol. 2, Topics in Photosynthesis (Barber, J., ed.), pp. 99—147, Elsevier/North Holland, Amsterdam
4 Arntzen, C.J. (1978) in Current Topics in Bioenergetics, Vol. 7, (Sanadi, D.R. and Vernon, L.P., ed.), pp. 111—160, Academic Press, New York
5 Gross, E.L. and Prasher, S.H. (1974) Arch. Biochem. Biophys. 164, 460—468
6 Vandermeulen, D.L. and Govindjee (1974) Biochim. Biophys. Acta 368, 61—70
7 Barber, J., Mills, J.D. and Love, A. (1977) FEBS Lett. 74, 174—181
8 Mills, J.D. and Barber, J. (1978) Biophys. J. 21, 257—272
9 Barber, J. and Searle, G.F.W. (1978) FEBS Lett. 92, 5—8
10 Chow, W.S., Thorne, S.W., Duniec, J.T., Sculley, M.J. and Boardman, N.K. (1980) Arch. Biochem. Biophys. 201, 347—355
11 Rubin, B.T. and Barber, J. (1980) Biochim. Biophys. Acta 592, 87—102
12 Barber, J. and Chow, W.S. (1979) FEBS Lett. 105, 5—10
13 Barber, J. (1980) FEBS Lett. 118, 1—10
14 Duniec, J.T., Sculley, M.J. and Thorne, S.W. (1979) J. Theor. Biol. 74, 473—484
15 Sculley, M.J., Duniec, J.T., Thorne, S.W., Chow, W.S. and Boardman, N.K. (1980) Arch. Biochem. Biophys. 201, 339—346
16 Barber, J. (1979) in Ciba Foundation Symposium (London) Vol. 61, pp. 283—304, Elsevier, Amsterdam
17 Barber, J., Chow, W.S., Scoufflaire, C. and Lannoye, R. (1980) Biochim. Biophys. Acta 591, 92—103
18 Chow, W.S. and Barber, J. (1980) Biochim. Biophys. Acta 593, 149—157
19 Hall, D.G. (1977) J.C.S. Faraday Trans. II 54, 101—112
20 Hall, D.G. and Sculley, M.J. (1977) J.C.S. Faraday Trans. II, 54, 869—876
21 Parsegian, V.A. and Ninham, B.W. (1973) J. Theor. Biol. 38, 101—109
22 Le Neveu, D.M., Rand, R.P., Parsegian, V.A. and Gingell, D. (1977) Biophys. J. 18, 209—229
23 Cowley, A.C., Fuller, N.L., Rand, A.P. and Parsegian, V.A. (1978) Biochemistry 17, 3163—3168
24 Bell, G.M. and Paterson, G.C. (1972) J. Colloid Interface Sci. 41, 542—566
25 Nir, S. and Bentz, J. (1978) J. Colloid Interface Sci. 65, 399—414
26 Mercer, F.V., Hodge, A.J., Hope, A.B. and McLean, J.D. (1955) Aust. J. Biol. Sci. 8, 1—18
27 Nakatani, H.Y., Barber, J. and Forrester, J.A. (1978) Biochim. Biophys. Acta 504, 215—225
28 Barber, J. and Searle, G.F.W. (1979) FEBS Lett. 103, 241—245
29 Itoh, S. (1978) Biochim. Biophys. Acta 504, 324—340

30 Chow, W.S. and Barber, J. (1980) Biochim. Biophys. Acta 589, 346—352
31 Berg, S., Dodge, S., Krogmann, D.W. and Dilley, R.A. (1974) Plant Physiol. 53, 619—627
32 Prochaska, L.J. and Gross, E.L. (1975) Biochim. Biophys. Acta 376, 120—135
33 Nir, I. and Pease, D.C. (1973) J. Ultrastruct. Res. 42, 534—550
34 Israelachvili, J.N. and Adams, G.E. (1978) J.C.S. Faraday Trans. I 74, 975—1001
35 Haynes, H.D., Kolber, M.A. and Morris, S.J. (1979) J. Theor. Biol. 81, 713—743
36 Israelachvili, J.N. (1978) in Light Transducing Membranes (Deamer, D.W., ed.), pp. 91—107, Academic Press, New York
37 Weinbaum, S. (1980) J. Theor. Biol. 83, 63—92
38 Staehelin, A.L. and Arntzen, C.J. (1979) in Ciba Foundation Symposium (New Series), Vol. 61, pp. 147—169, Excerpta Medica, Amsterdam
39 Richmond, P. (1975) in A Specialist Periodical Report, Colloid Science, Vol. 2 (Everett, D.H., Senior Reporter), The Chemical Society
40 Olivares, W. and McQuarrie, D.A. (1980) J. Phys. Chem. 84, 863—867
41 Richmond, P. (1975) J. Chem. Soc. Far. Trans. II 71, 1154—1163